School of Mechanical Engineering Faculty Publications

School of Mechanical Engineering

2009

The Effect of Polydispersivity on the Thermal Conductivity of Particulate Thermal Interface Materials

Sasanka Kanuparthi

Ganesh Subbarayan

Thomas Siegmund
Purdue University, siegmund@purdue.edu

Bahgat Sammakia

Follow this and additional works at: http://docs.lib.purdue.edu/mepubs

Part of the Mechanical Engineering Commons

The Effect of Polydispersivity on the Thermal Conductivity of Particulate Thermal Interface Materials

1
2
3
4
5
6
7
8
9
10
11
12
13
14
15
16
17
18
19
20
21
22
23
24
25
26
27
28
29
30
31
32
33
34
35
36
37
38
39
40
41
42
43
44
45
46
47
48
49
50
51
52
53
54
55
56
57
58
59
60

The Effect of Polydispersivity on the Thermal Conductivity of Particulate Thermal Interface Materials

S. Kanuparthi[1], G. Subbarayan[1+], T. Siegmund[1] and B.G. Sammakia[2]

[1]School of Mechanical Engineering, Purdue University, West Lafayette, IN 47906

[2]Watson School of Engineering, State University of New York, Binghamton, NY 13902

[+] Tel: (765) 494-9770   Email: ganeshs@purdue.edu

1

Abstract

A critical need in developing thermal interface materials (TIMs) is an understanding of the effect of particle/matrix conductivities, volume loading of the particles, the size distribution, and the random arrangement of the particles in the matrix on the homogenized thermal conductivity. Commonly, TIM systems contain random spatial distributions of particles of a polydisperse (usually bimodal) nature. A detailed analysis of the microstructural characteristics that influence the effective thermal conductivity of TIMs is the goal of this paper. Random microstructural arrangements consisting of lognormal size-distributions of alumina particles in silicone matrix were generated using a drop-fall-shake algorithm. The generated microstructures were statistically characterized using the matrix-exclusion probability function. The filler particle volume loading was varied over a range of 40-55 %. For a given filler volume loading, the effect of polydispersivity in the microstructures was captured by varying the standard deviation(s) of the filler particle size distribution function. For each particle arrangement, the effective thermal conductivity of the microstructures was evaluated through numerical simulations using a network model previously developed by the authors. Counter to expectation, increased polydispersivity was observed to increase the effective conductivity up to a volume loading of 50%. However, at a volume loading of 55%, beyond a limiting standard deviation of 0.9, the effective thermal conductivity decreased with increased standard deviation suggesting that the observed effects are a trade-off between resistance to transport through the particles versus transport through the inter-particle matrix gap in a percolation chain.

2

1
2
3
4
5
6
7
8
9
10
11
12
13
14
15
16
17
18
19
20
21
22
23
24
25
26
27
28
29
30
31
32
33
34
35
36
37
38
39
40
41
42
43
44
45
46
47
48
49
50
51
52
53
54
55
56
57
58
59
60

Keywords: Thermal interface materials, network models, polydispersvitiy.

Nomenclature

f	probability density function
D	particle diameter
m	positive integer
C	cumulative distribution function
N	number of particles of a given size
N_{reqd}	required number of particles of a given size
V_{ini}	total volume of the particles
V_{reqd}	required volume of the particles
h_v	matrix nearest-surface distribution function
e_v	matrix exclusion probability function
r_o	distance from a matrix point to the nearest particle surface
k_m	thermal conductivity of the base (polymer) matrix, [W/mK]
k_p	thermal conductivity of the filler material particles, [W/mK]
n	number of particles simulated in the microstructure

Greek symbols

Γ	gamma function
μ	mean logarithm of the particle diameter
σ	standard deviation of the logarithm of the particle diameter (polydispersivity parameter)
Δ	particle size increment

3

Φ_2 volume fraction of spheres in the microstructure

η, θ Weibull parameters

β, ε network model parameters

Subscripts

avg   mean particle diameter

min   minimum particle diameter

ini, fin   limiting particle size diameters

unit   unit cell volume

reqd   final required number of particles

m   matrix

p   filler particle

TC   thermal conductivity

Abréviations

TIM   Thermal Interface Material

SC   Self-consistent Approximation

BAM   Bruggeman Assymetric Model

Introduction

Polydispersivity in the size-distribution of the constituent particles is a fundamental microstructural feature in a wide range of technological applications. These applications include propellants made of composite solids [1], colloids [2], sintering of powders [3], mechanical properties and transport phenomena of particulate composite materials [4], and flow in packed beds [5]. Thus, there is a widespread interest in understanding the effect of polydispersivity of the constituent particles on the effective properties of the microstructures. However, there is little work in the literature to systematically relate polydispersivity to effective behavior. The particular application of interest in this paper is the thermal transport in particulate composites. The effective thermal behavior of particle laden polymeric materials depend, in addition to particle/matrix conductivities and volume loading of the particles, on the randomness of distribution, on the randomness of the size as well as on the interfacial thermal resistance between the particles and the matrix.

The classical models such as the Maxwell's model [6] are extensions of "single-particle" models and treat particles as being well separated. That is, they ignore inter-particle interactions. The extensions to Maxwell's model include those that have introduced imperfect interfacial contact [7] as well as those that have modeled non-spherical particles [8]. Benvensite [9] obtained the same result as Hasselman et al. [7] based on a micromechanics (Mori-Tanaka based) approach. These models are applicable only when the particles are well separated from one-another. Another drawback in the above models is that they do not account for the random microstructural arrangements

with their resulting inter-particle interactions, or the polydispersivity of the inclusions. The model by Rayleigh [10] attempts to capture the inter-particle interaction through a simple cubic cellular arrangement of identical particle sizes. While this leads to an improved estimate, the model is incapable of capturing the effects of random size distribution or random arrangement. Extensions to Rayleigh's model include those that have allowed other alternative periodic arrangements (to the simple cubic arrangement) such as face-centered cubic and body-centered cubic cells [11, 12] as well as those that have studied the effective behavior of particles in near contact [13]. There is an inherent assumption of the spheres being "well separated" from one another in these models as well [14].

Another popular method of estimating the effective thermal conductivity of composites is using the self-consistent (SC) approximation, which was originally developed by Bruggeman [15] and further extended by Landauer [16, 17]. The method is based on the approximation that the medium outside a particular type of inclusion can be considered to be homogeneous, the effective conductivity of which needs to be determined. SC approximations do not account for the spatial distribution of the inclusions and are of questionable validity when applied to systems that do not posses phase-inversion symmetry [14]. The fundamental assumption of the existence of an effective medium outside of a "test" sphere is invalid when identical spheres are packed. The SC approximation also fails when applied to composites with widely different phase thermal conductivities [14].

The asymmetric differential effective-medium approximation scheme was also developed by Bruggeman [15]. Bruggeman assumed that the filler material particles were

6

added progressively to a composite matrix whose effective behavior is known at any given stage. Every et al. [18] used Bruggeman's asymmetric model (BAM) for predicting the effective thermal conductivity of ZnS/Diamond composites. The deficiencies of using the BAM for predicting the composite thermal conductivity are described in [19].

The goal of the present paper is to study the effect of polydispersivity on the effective thermal transport in polymeric composites using a computationally efficient random network model developed earlier by the authors [20, 21]. The network model was demonstrated in our prior work to capture accurately (for composites with a very high contrast in the constituent thermal conductivities) the effect of random spatial distribution of the particles as well the constituent thermal conductivities on the effective thermal conductivity of the composite. Such models are needed at intermediate and large volume fractions where classical analytical models that assume "dilute limits" are not accurate.

The network model used in the present study was verified in our prior work against exhaustive full-field simulations using a sophisticated meshless computational tool [22]. The full-field models themselves were verified in our prior work against experimentally measured effective conductivity values on systems consisting of alumina as well as aluminum in epoxy matrix [19]. Therefore, in the present work, the focus is on studying the effect of polydisersivity using the network model. Here, the size distribution of the filler particles is assumed to follow a lognormal probability density function. The effect of polydispersivity is captured by varying the standard deviation parameter in the lognormal filler particle size distribution function. Lastly, important guidelines for enhancing the effective thermal conductivity of particulate composites are presented.

7

Microstructure Generation

The size distribution of the filler particles is generally characterized using normalized probability density functions. There is a wide variety of size distribution functions that can be used to characterize physical phenomena. However, two of the more commonly used probability density functions are the *Schulz* [23] and the *log-normal* [24] distribution functions. The Schulz distribution function is defined as:

$$f(D) = \frac{1}{\Gamma(m+1)} \left(\frac{m+1}{\langle D \rangle} \right)^{m+1} D^n \exp\left[\frac{-(m+1)D}{\langle D \rangle} \right] \tag{1}$$

where, f is the probability density function, D is the particle diameter and $\Gamma(m+1)$ is the gamma function. When m is restricted to positive integer values, $\Gamma(m+1) = m!$. The two extremes of the distribution function are obtained by setting $m = \infty$, which is the monodisperse limit (uniform sized particles), and $m = 0$, which corresponds to the other extreme of highly polydisperse limit (exponential function) in which many particles have extremely small radii.

The log-normal distribution function is defined as:

$$f(D) = \frac{1}{D\sqrt{2\pi\sigma^2}} \exp\left\{ -\frac{[\ln(D) - \mu]^2}{2\sigma^2} \right\} \tag{2}$$

$$C(D) = \frac{1}{2} + \frac{1}{2} erf\left[\frac{\ln(D) - \mu}{\sigma\sqrt{2}} \right] \tag{3}$$

where, f is the probability density function, C is the cumulative distribution function, D is the particle diameter and μ and σ are the mean and standard deviation of the variable's (particle diameter D in this case) logarithm.

The log-normal distribution function is used to generate microstructures with varying degree of polydispersivity in this paper. This is since the lognormal distribution is versatile in being able to capture a wide variety of distributions (see Figure 1). The mean particle diameter is assumed to be 1 and the unit cell size of the microstructures is assumed to 5 x 5 x 5 (unit cell side being equal to five times the mean particle diameter). The effect of polydispersivity was systematically captured by varying the σ value in Eq. (2). The following σ values were considered: 0.1, 0.9, 1.2 and 2, to generate the microstructures. The log-normal probability density functions used to describe the particle size distributions in the simulated microstructures are shown below in Figure 1. As can be seen from the figure, for small values of standard deviation, the log normal distribution approximates the normal distribution and is versatile in its ability to model different forms of density functions. The simulations were performed for varying filler volume loadings of: 40, 45, 50 and 55 % respectively. These volume loadings represent intermediate values that have practical significance for TIM applications, and values at which assumptions of "dilute fractions" no loner hold.
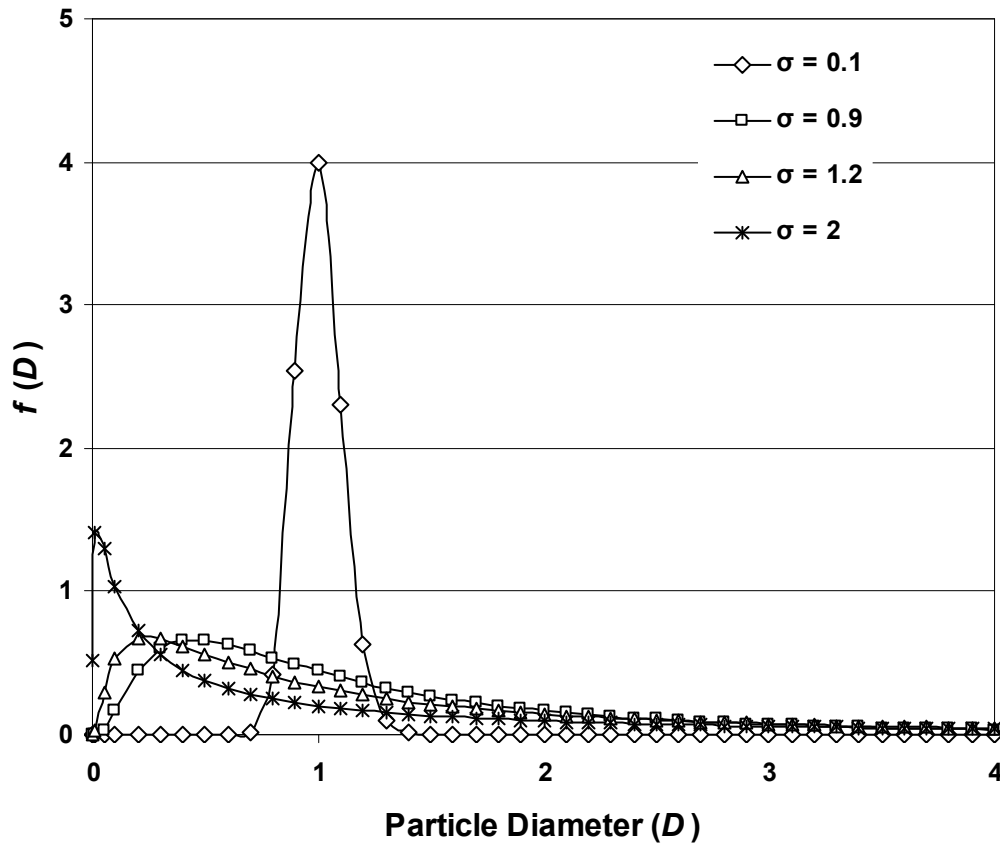
9

Figure 1: Lognormal probability density functions used to describe particle size distribution for $\mu = \ln(1) = 0$ and $\sigma = 0.1, 0.9, 1.2$ and 2.

As mentioned earlier, the mean particle diameter was assumed to be unity. That is, $D_{avg}=1$. A unit cell of size 5 x 5 x 5 was used in the simulations.

The following procedure was used to generate the microstructures:

1. The minimum particle size diameter (D_{min}) considered was equal to 0.1 (one-tenth of the mean particle diameter). The particle size was incremented in steps of $\Delta D = 0.1$. Therefore, the particle sizes (diameters) considered were 0.1, 0.2, 0.3,……, 1, 1.1, 1.2… and so on. For a given σ value, the particle sizes were restricted to within the range where $f(D)$ was greater than zero by a chosen tolerance. For example, for $\sigma = 0.1$, the particle sizes were restricted between 0.7

10

− 1.4 as seen in Figure 1. This was done to eliminate particle sizes that have nearly zero frequency of occurrence, and thereby ensuring that the number of particles in the simulation is the smallest required to capture the physical phenomenon.

2. The number of particles of a given size $N(D)$ was calculated based on the cumulative distribution function values as shown below:

$$N(D) = C\left(D + \frac{\Delta D}{2}\right) - C\left(D - \frac{\Delta D}{2}\right) \tag{4}$$

3. The total volume of the particles was then calculated based on $N(D)$. This is referred to as V_{ini} and was calculated as follows:

$$V_{ini} = \sum_{D=D_{ini}}^{D=D_{fin}} N(D) \times \frac{4}{3}\pi\left(\frac{D}{2}\right)^3 \tag{5}$$

where, D_{ini} and D_{fin} refer to the limiting particle size diameters for a given σ value. For example, for $\sigma = 0.1$, $D_{ini} = 0.7$ and $D_{fin} = 1.4$.

4. The required volume V_{reqd} of the particles was estimated based on the desired volume loading of the microstructures. For example, if one requires a microstructure with a 40% filler volume loading, based on the unit cell volume of $V_{unit} = 5 \times 5 \times 5 = 125$, $V_{reqd} = 0.4 \times 125 = 50$.

5. The final required number of particles of a given size $N_{reqd}(D)$ was then calculated as follows:

$$N_{reqd}(D) = \left(\frac{V_{reqd}}{V_{ini}}\right) N(D) \tag{6}$$

11

6. Given the number of filler particles of each size $N_{reqd}(D)$ from step 5 above, the drop-fall-shake algorithm earlier developed [25, 26, 27] in a java-based simulation was used to generate the various microstructures. The procedure is illustrated in Figure 2. Given the filler particle size distribution, the particles are initially randomly arranged inside a larger unit cell starting from the larger particle to the smallest. The particles are then dropped to the bottom of the unit cell starting from the particle closest to the bottom of the unit cell and sequentially proceeding to the farthest particle from the bottom of the unit cell. Each particle is dropped many number of times from various random positions in the X-Y plane to ensure that the particle reaches the bottom most possible position in the unit cell. The size of the unit cell is then reduced to achieve a specific filler volume loading. The particles are then randomly selected and moved either to the bottom of the unit cell or to the top of the unit cell with a probability of 0.5. This procedure ensures that the particles are randomly and uniformly distributed in the final unit cell with the prescribed volume fraction. For a given filler volume loading and σ value, *thirty different microstructures* were generated to achieve statistical confidence in estimates.

7. For higher σ values and high filler volume loadings, the size of the unit cell (and proportionally the number of particles) had to be increased to ensure that all the filler particles fit inside the unit cell. The motivation for this was computational in achieving a microstructure with a given volume fraction than something that was dictated by the physics of the problem. The unit cell was grown incrementally in

all three directions to achieve this. The sizes of the unit cells simulated ranged

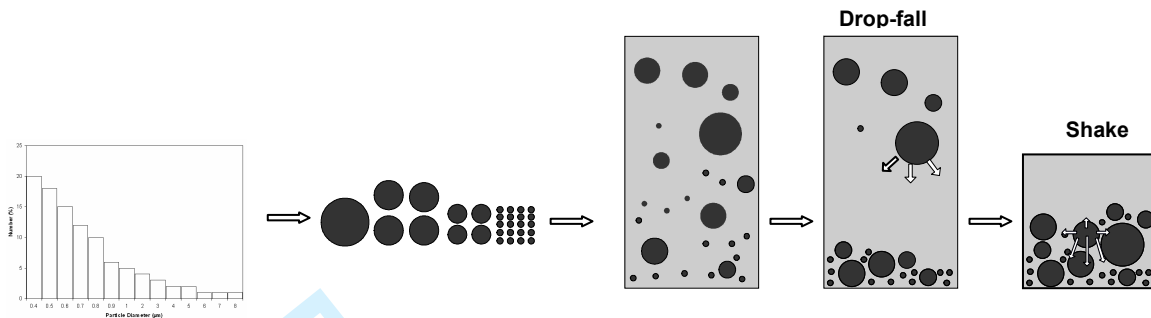from 10 x 10 x 10 all the way to 120 x 60 x 60.

Figure 2: An illustration of the drop-fall-shake algorithm used to generate polydisperse
microstructures.

Statistical Characterization of Microstructures

There are wide variety of statistical descriptors for characterizing random two-
phase microstructures in the literature [14 and references there within] namely: i) N-point
probability function ii) Surface-correlation function iii) Lineal-path function iv) Chord-
length density function v) Pore-size function vi) Percolation and Cluster functions vii)
Nearest-neighbor functions viii) Point/q-particle correlation function and ix) Surface-
particle function.

Among the available formalisms, the nearest-neighbor functions are commonly
used for characterizing particulate dispersions. These are of two types namely: nearest-
surface distribution functions and nearest-center distribution functions. For example in
Figure 3, particle 1 has the nearest center to the point A, whereas particle 2 has the
nearest surface. In particular, for characterizing polydispersed systems, nearest-surface
distribution functions are more relevant than the nearest-center distribution functions

13

[28]. This is particularly true in the context of particulate thermal interface materials since the effective thermal conductivity of these high volume loading composites depend highly non-linearly on the interparticle gaps (nearest surface distances between the filler particles) as argued by Batchelor and O'Brien [29].
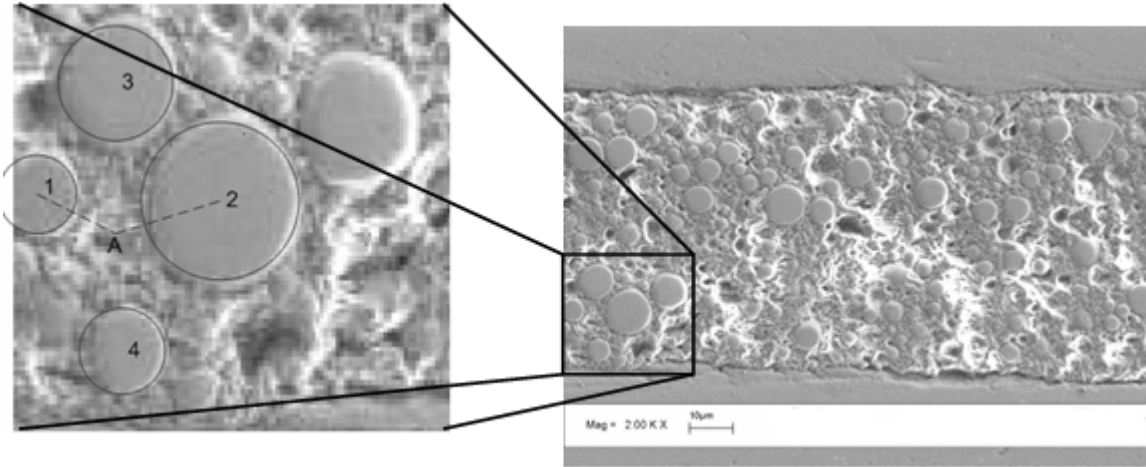

Figure 3: Interpretation of nearest-surface and nearest center distribution functions.

The matrix nearest-surface distribution function $h_v(r_o)$ (see Figure 4) is defined such that $h_v(r_o)dr_o$ is the probability that the nearest particle surface lies at a distance between r_o and $r_o + dr_o$, from an arbitrary matrix point (points in the microstructure lying exterior to the particles in the matrix region) in the microstructure. The corresponding matrix exclusion probability function $e_v(r_o)$ is associated with the complementary cumulative distribution function of $h_v(r_o)$ as:

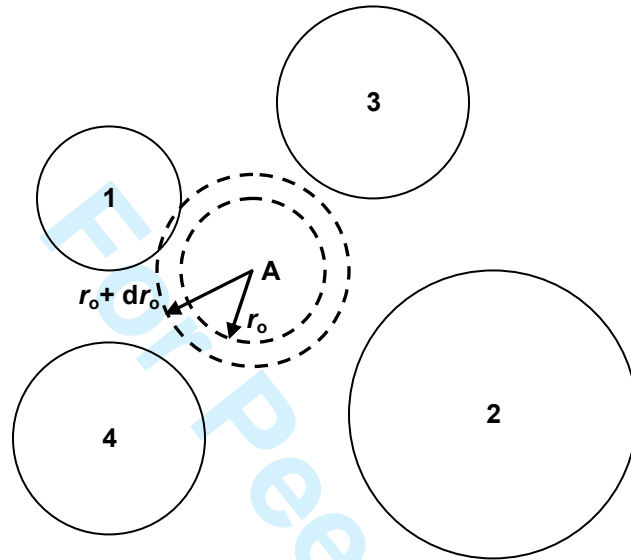$$e_v(r_o) = 1 - \int_{-\infty}^{r_o} h_v(x)dx \qquad (7)$$

14

Figure 4: Schematic representation of matrix-nearest surface distribution function.

Figure 5 illustrates the exclusion probability function $e_v(r_o)$ plots for two limiting cases of Schulz distribution function for highly polydisperse ($m = 0$) and monodisperse ($m = \infty$) systems consisting of hard spheres in equilibrium at the same volume fraction of $\Phi_2 = 0.2$. As seen from Figure 5, the exclusion probability function $e_v(r_o)$ increases with increase in the degree of polydispersivity. Physically, this means that there is a higher probability of finding a larger matrix region in the polydisperse scenario in comparison to the monodisperse case.
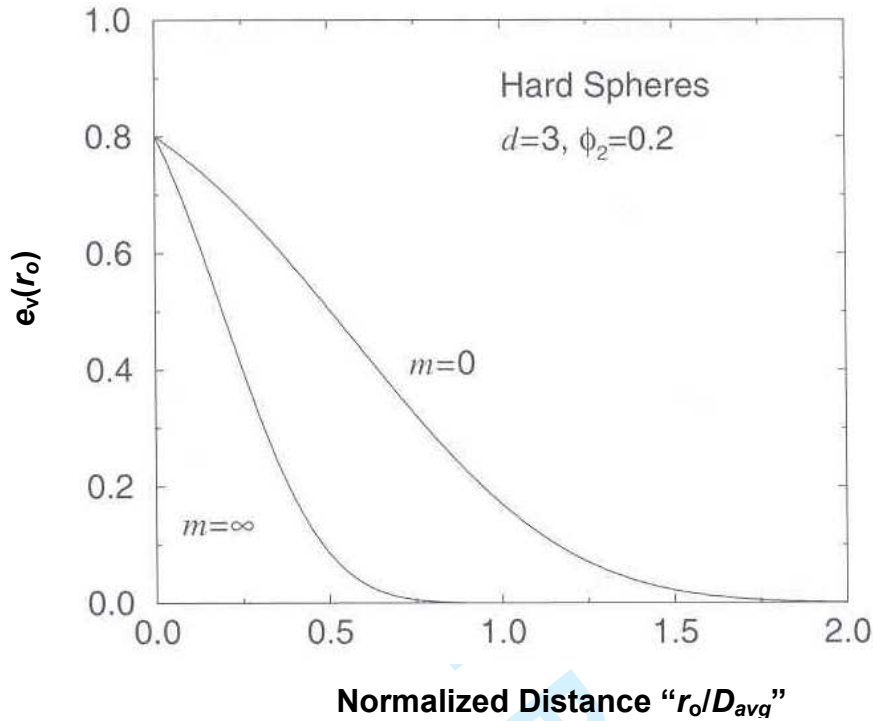
15

Figure 5: Matrix-exclusion probability function versus normalized distance. The distance is normalized with respect to the mean diameter "D_{avg}" of the particles (adapted from [14]).

The matrix exclusion probability was evaluated by considering $\sim 10^6$ arbitrary matrix points for *each* of the microstructures. The matrix points were surrounded with concentric shells of radii $r_o = i\Delta r$, $i = 1,2,3......$, and thickness Δr (where $\Delta r <<$ particle radii). For each matrix point, the particle that had the nearest surface distance was found and the corresponding distance was recorded. Subsequently, the number of shells (for a given shell radius r_o) containing the nearest surface points were counted as successes. For a given shell radius, the number of successes divided by the total number of matrix points

16

gives the probability $h_v(r_o)dr_o$ for that particular shell radius between r_o and $r_o + dr_o$. From the $h_v(r_o)$ versus r_o plot, the matrix exclusion probability function $e_v(r_o)$ can be calculated using Eq. (7) and multiplying it with the volume fraction of the matrix space in the microstructure. The probability plots for all the microstructures were generated and were fit using a Weibull distribution for the matrix nearest-surface distribution function $h_v(r_o)$ as shown below:

$$h_v(r) = \eta\theta^{-\eta}r^{\eta-1}e^{-\left(\frac{r}{\theta}\right)^{\eta}} \tag{8}$$

Microstructure-Property Relationship

The details of all the simulated microstructures are listed in Table 1. The properties of the polymer matrix–filler particle combinations used in the simulations were: Silicone matrix – (k_m = 0.2 W/mK), Alumina filler (k_p = 25 W/mK). For volume loadings 40%, 45% and 50%, the degree of polydispersivity was varied between 0.1, 0.9 and 2. For volume loading of 55%, the degree of polydispersivity was varied between 0.1, 0.9 and 1.2. This was since it was progressively more difficult to generate as well as simulate microstructures with higher degree of polydispersivity at higher filler volume loadings. As the number of particles "n" simulated in the microstructure increases, the computational time for matrix inversion calculations in the network model increases as $\sim n^3$. The size of the microstructures was also increased accordingly in the X, Y and Z directions to achieve microstructures with all particles inside the simulation boundary. A total of thirty simulations were carried out for a given σ and volume loading since it is

17

known that large number of repetitions (commonly $N \geq 30$) enable one to approximate

the estimate of the mean as a normal distribution with a standard deviation of $\dfrac{\sigma}{\sqrt{N}}$ [30].

The mean and standard deviation (obtained by simulating thirty different microstructures)

of the (normally distributed) Weibull parameters η and θ obtained for all the different

systems simulated are shown in Table 2. The mean matrix nearest-surface exclusion

volume probability functions characteristic of the different systems simulated along with

the representative unit cells are shown in Figures 6 – 13.

Table 1: Parameters describing the simulated microstructures.

Filler Volume Loading (%)	σ	N *	Unit Cell Size	Particle Diameter Range	Total # Particles
40	0.1		10 x 10 x 10	0.7 - 1.4	728
	0.9		15 x 15 x 15	0.1 - 5.4	350
	2		30 x 30 x 30	0.1 - 9.4	299
45	0.1		10 x 10 x 10	0.7 - 1.4	820
	0.9		30 x 30 x 30	0.1 - 5.6	3128
	2		60 x 60 x 60	0.1 - 9.7	2664
50	0.1	30	15 x 15 x 15	0.7 - 1.4	3073
	0.9		30 x 30 x 30	0.1 - 5.6	3520
	2		75 x 60 x 60	0.1 - 9.9	3690
55	0.1		30 x 15 x 15	0.7 - 1.4	6762
	0.9		60 x 22.5 x 22.5	0.1 - 5.6	4329
	1.2		120 x 60 x 60	0.1 - 9.9	9152

* Represents the number of microstructures simulated for each σ value for a given filler volume loading

18

Table 2: Characteristic Weibull distribution parameters of the simulated microstructures.

Filler Volume Loading (%)	σ	$\eta\ (\mu, \sigma_\eta)$	$\theta\ (\mu, \sigma_\theta)$
40	0.1	(1.25, 0.01)	(0.17, 0.00)
	0.9	(1.15, 0.03)	(0.50, 0.02)
	2	(1.14, 0.02)	(1.21, 0.04)
45	0.1	(1.19, 0.01)	(0.15, 0.00)
	0.9	(1.12, 0.05)	(0.43, 0.02)
	2	(1.12, 0.02)	(1.03, 0.04)
50	0.1	(1.18, 0.01)	(0.12, 0.00)
	0.9	(1.08, 0.02)	(0.36, 0.01)
	2	(1.10, 0.01)	(0.90, 0.01)
55	0.1	(1.16, 0.01)	(0.11, 0.00)
	0.9	(1.07, 0.02)	(0.31, 0.00)
	1.2	(1.07, 0.00)	(0.75, 0.00)

19

(a)

(b)

(c)

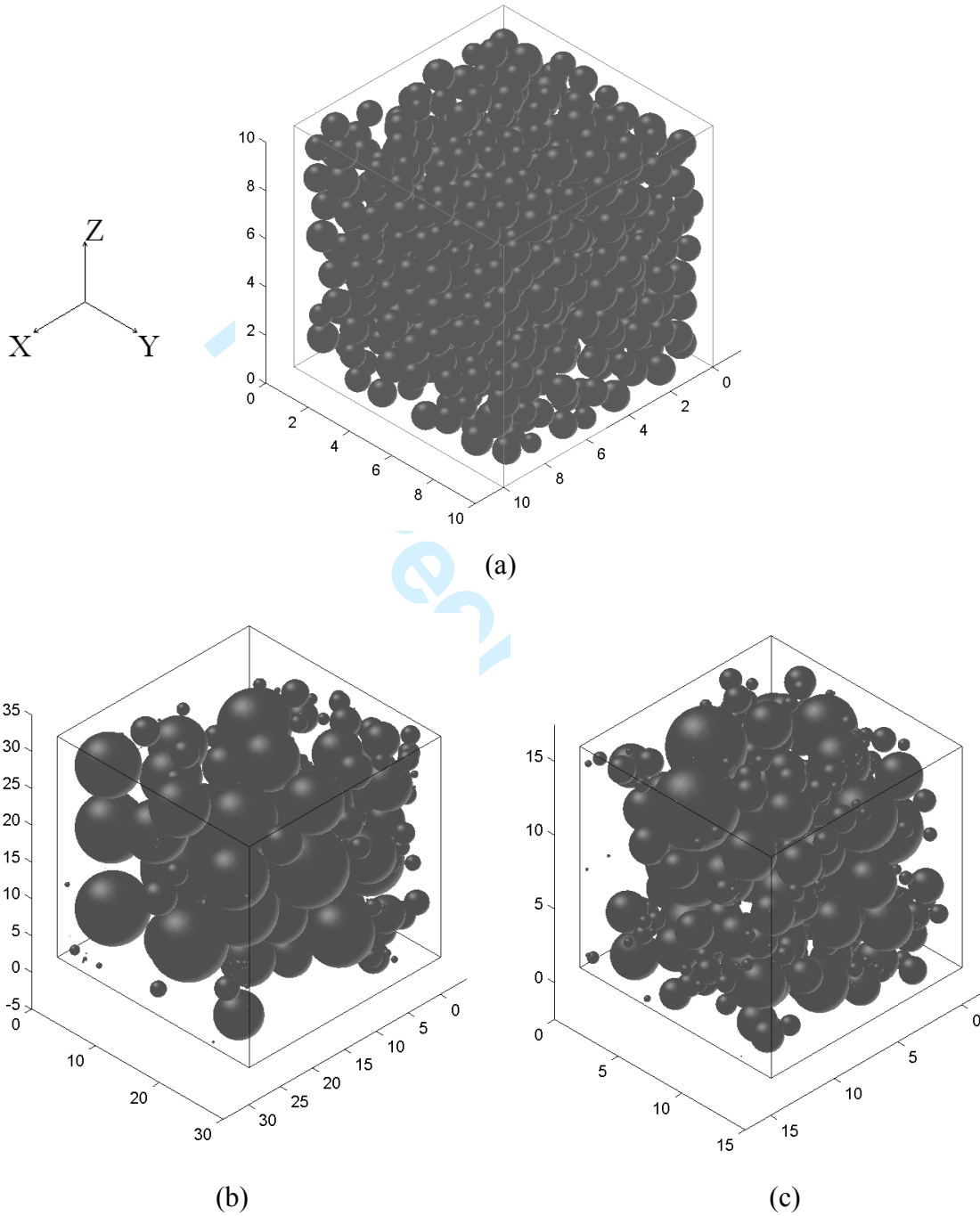Figure 6**:** Representative unit cells corresponding to a) $\sigma = 0.1$ b) $\sigma = 0.9$ and c) $\sigma = 2$ for 40% filler volume loading.
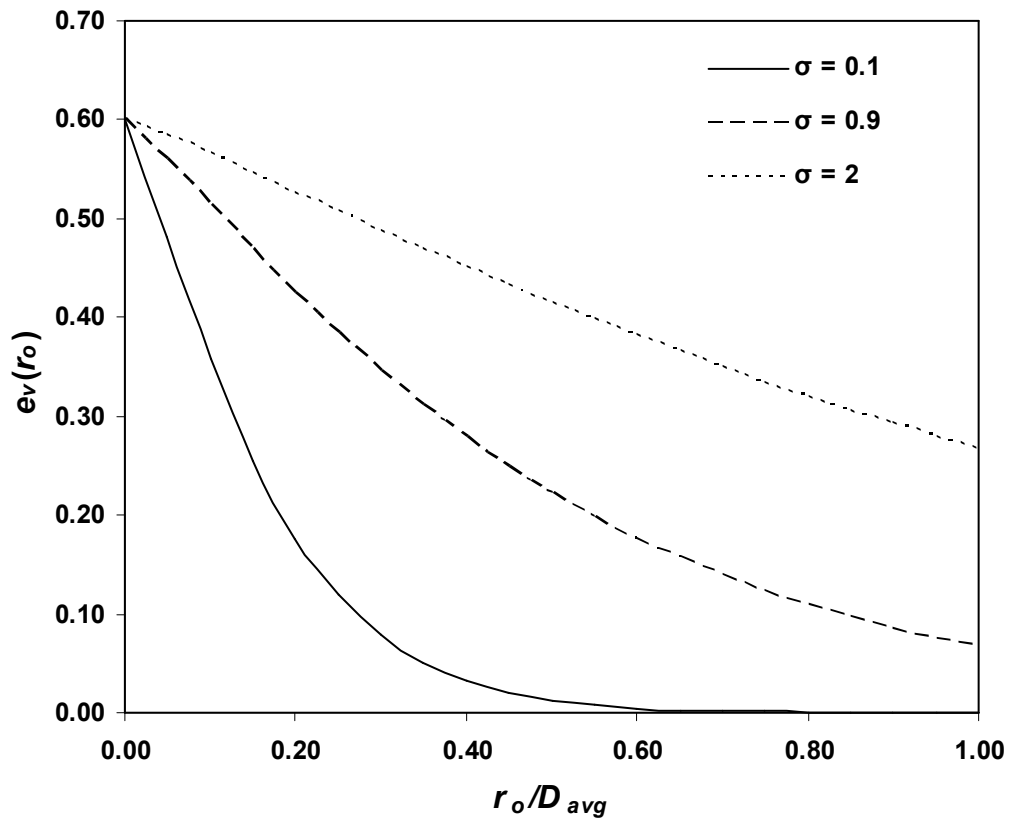
20

Figure 7: Mean characteristic void exclusion probability function $e_v(r_o)$ of the microstructures. The volume loading of the filler particles in the microstructures is 40%.
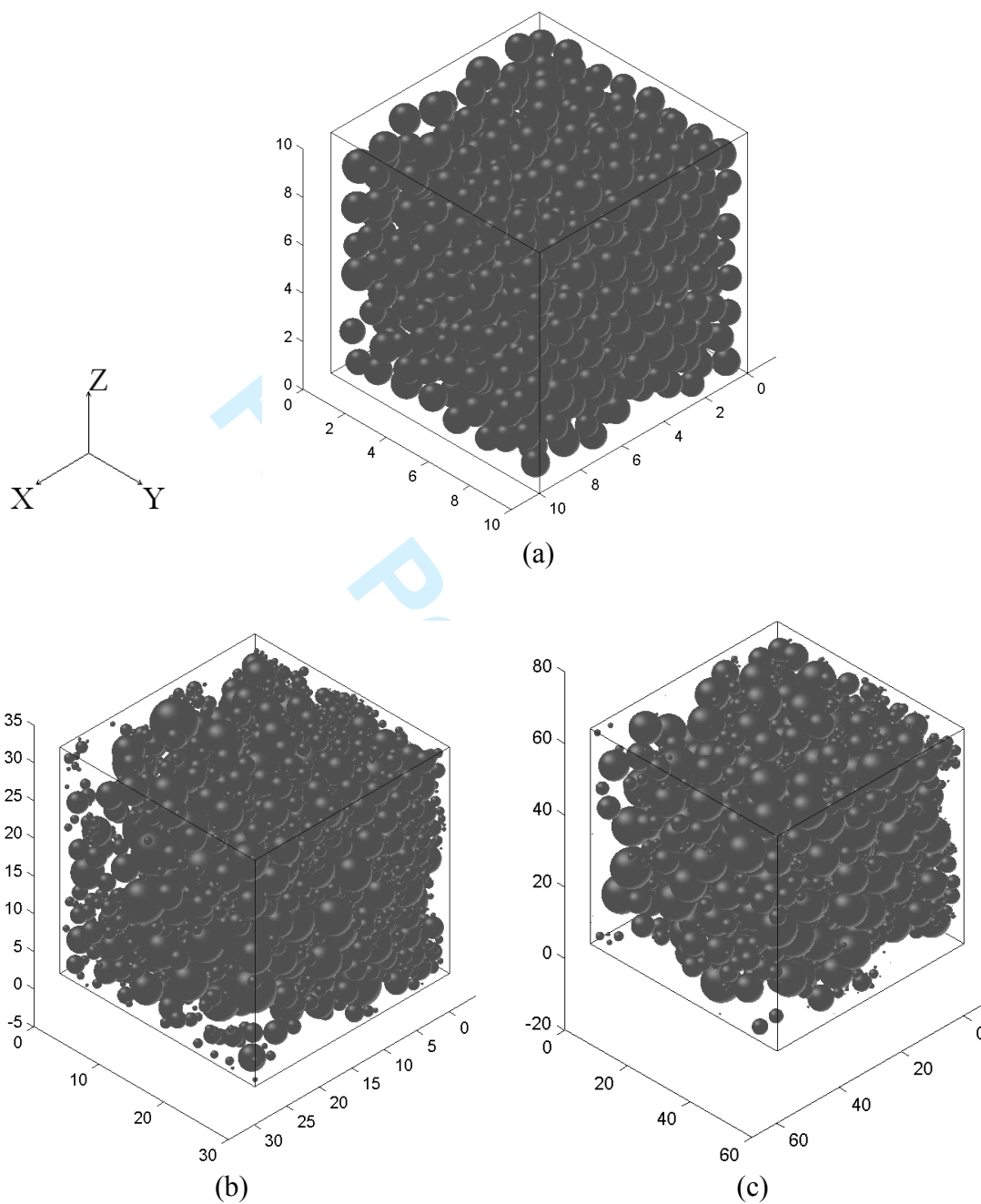
Figure 8: Representative unit cells corresponding to a) $\sigma = 0.1$ b) $\sigma = 0.9$ and c) $\sigma = 2$ for 45% filler volume loading.
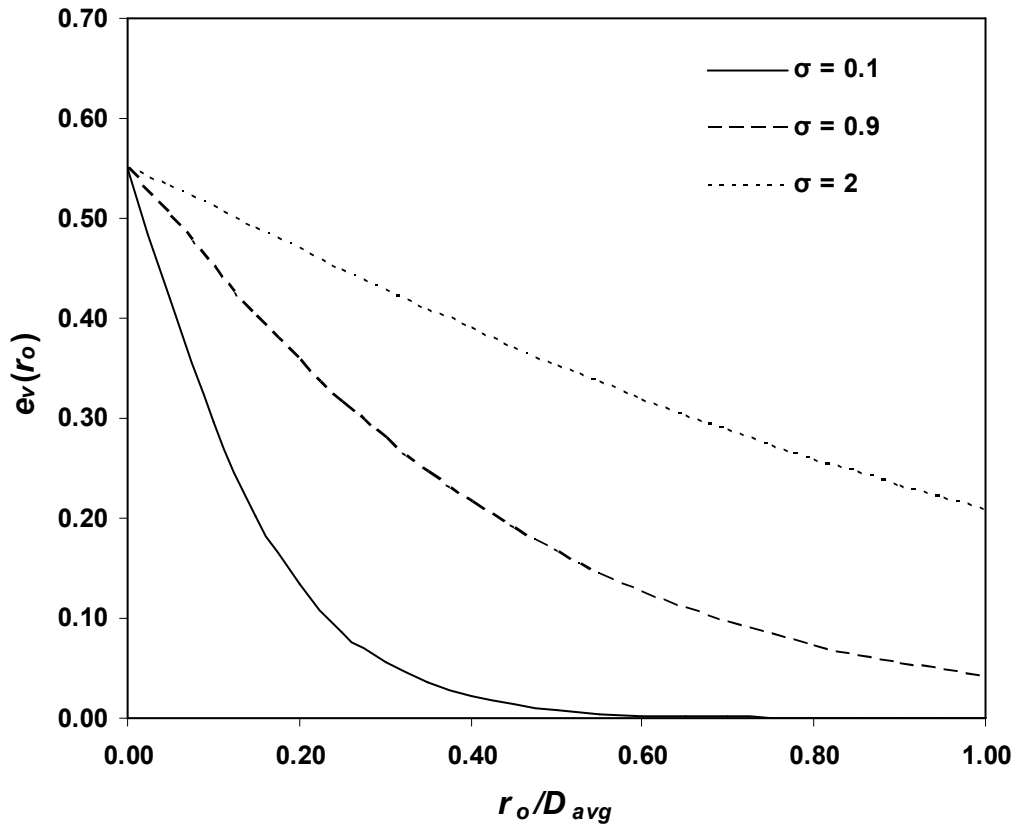
22

Figure 9: Mean characteristic void exclusion probability function $e_v(r_o)$ of the microstructures. The volume loading of the filler particles in the microstructures is 45%.
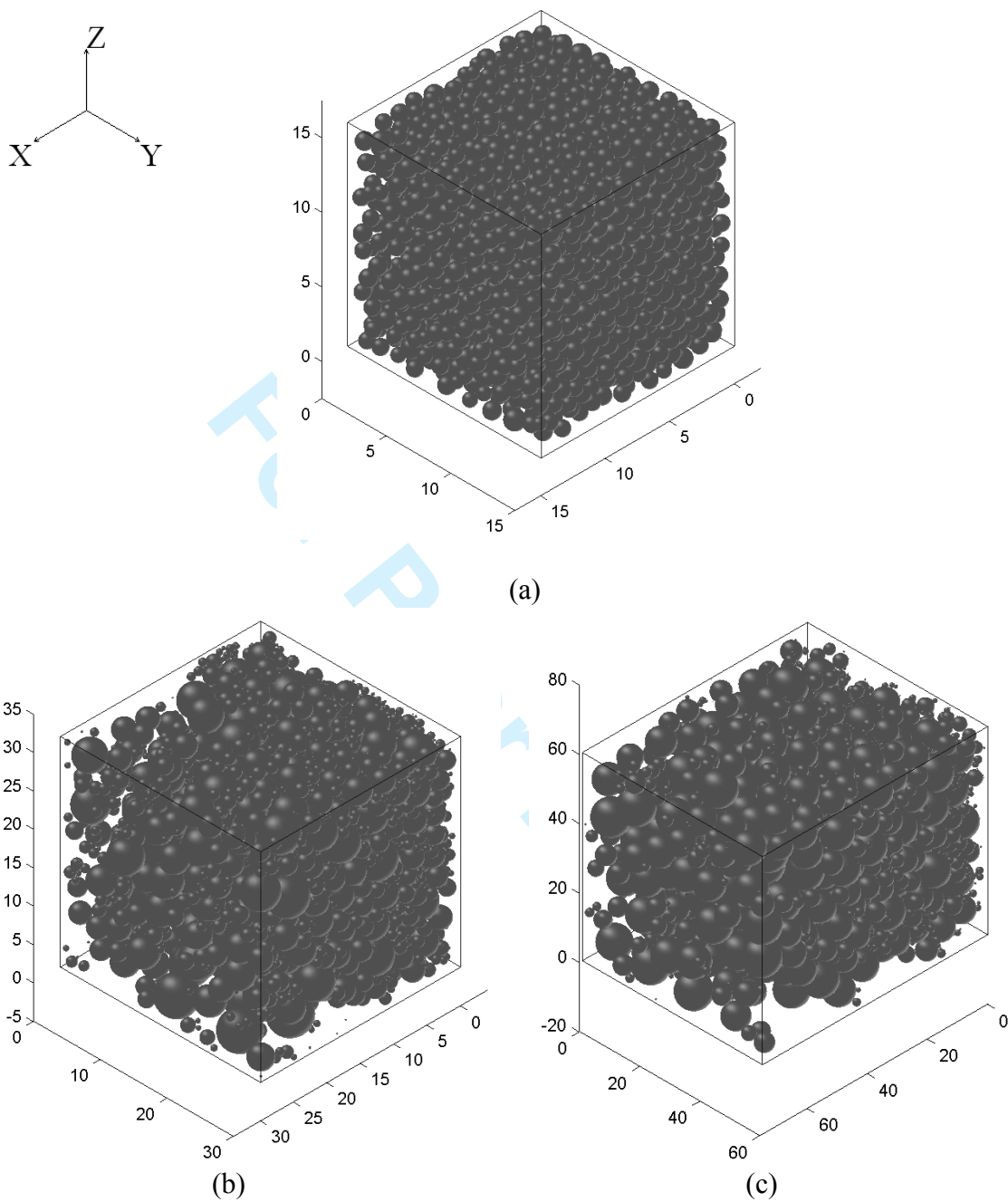
23

(a)

(b)

(c)

Figure 10: Representative unit cells corresponding to a) $\sigma = 0.1$ b) $\sigma = 0.9$ and c) $\sigma = 2$ for 50% filler volume loading.

Figure 11: Mean characteristic void exclusion probability function $e_v(r_o)$ of the microstructures. The volume loading of the filler particles in the microstructures is 50%.

Figure 12: Representative unit cells corresponding to a) $\sigma = 0.1$ b) $\sigma = 0.9$ and c) $\sigma = 1.2$ for 55% filler volume loading.
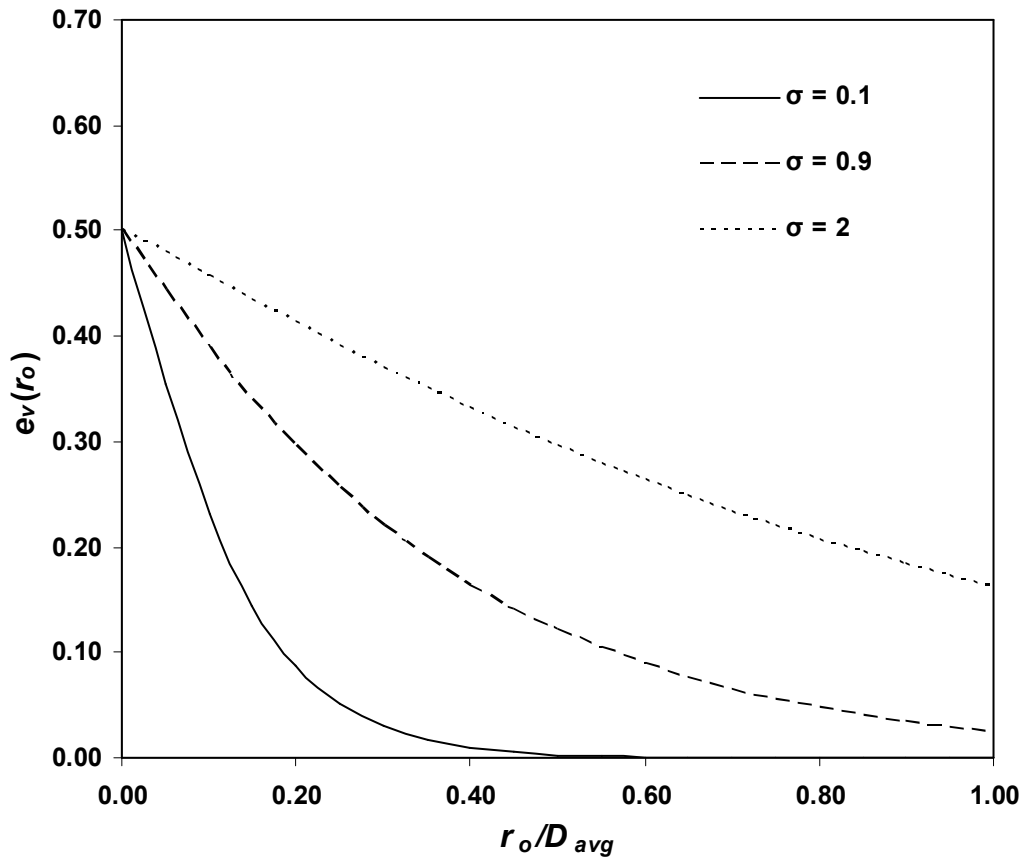
26

Figure 13: Mean characteristic void exclusion probability function $e_v(r_o)$ of the microstructures. The volume loading of the filler particles in the microstructures is 55%.
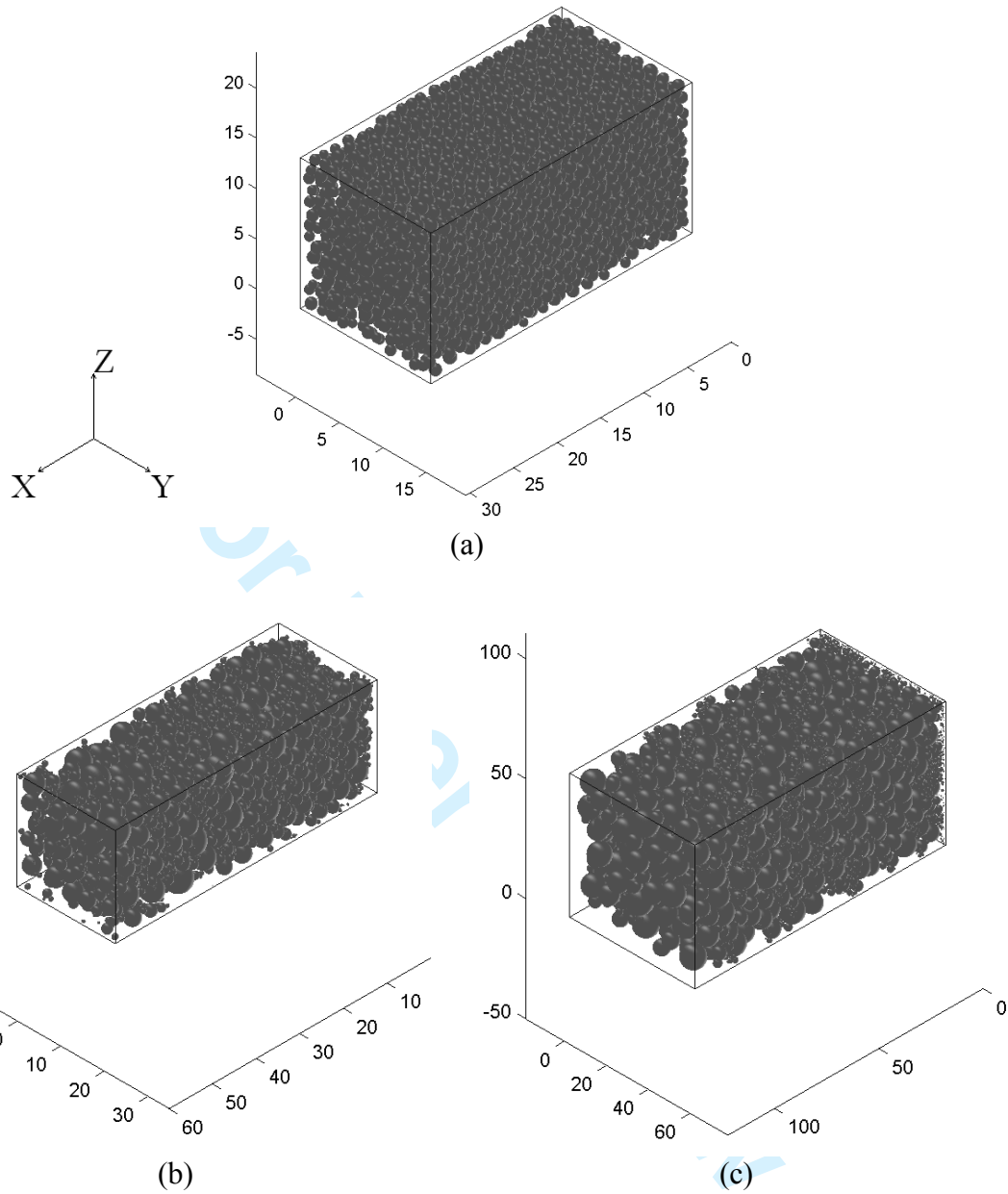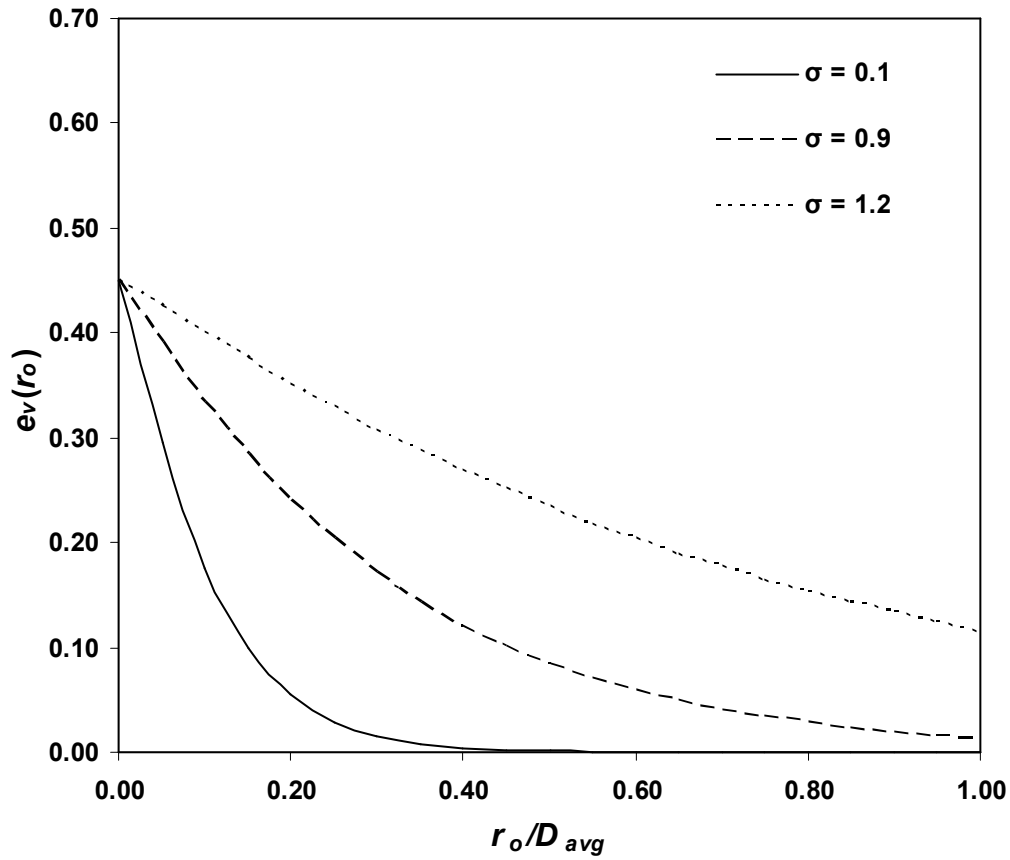
Results and Discussion

The thermal conductivities of the microstructures were evaluated using the network model earlier developed by the authors [20]. The network model parameters β and ε were kept at a constant value of 0.5 for all the simulations in this paper. Three-hundred and sixty simulations (thirty microstructures for a given filler volume loading and degree of polydispersivity σ value) were performed in all and the results are shown in Figures 14 – 17 for volume loadings ranging from 40–55%. Figure 18 summarizes the effect of polydispersivity on the thermal conductivity of the microstructures. The mean and standard deviation of the effective thermal conductivity of the composites for all the simulated microstructures are tabulated in Table 3.

As seen from Figures 14 – 16, increasing the degree of polydispersivity increases the effective thermal conductivity of the composites until 50% filler volume loading. However, for higher filler volume loading of 55%, the effective thermal conductivity increases until $\sigma = 0.9$, and then decreases for $\sigma = 1.2$ as seen in Figure 17. The statistical t-test results show that the mean thermal conductivity values for varying σ values (for a given filler volume loading) are statistically significantly different at a 95% confidence level. The t-test results and are summarized in Table 4. The important conclusions that can be drawn based on these results are as follows:

- Increasing the polydispersivity (σ value) increases the average size of the void regions in the microstructures as illustrated in Figure 5. Therefore, one would expect the effective thermal conductivity of the composites to decrease with the increasing σ value. In other words, a uniform-size distribution ($\sigma \to 0$) should

28

result in microstructures with the best thermal performance. However, the trends observed in this study are counter-intuitive. The primary reason for the increase in the effective thermal conductivity of the particulate composites with increasing σ value appears to be the reduced resistance to thermal transport in the particulate chains with higher degree of polydispersivity. In other words, the resistance to thermal transport through a larger particle is less than the combined resistance through a number of smaller particles. The polydispersivity also aids the formation of particle chains or the percolation. However, this trend cannot continue indefinitely since the effective surface area available for thermal transport decreases with increasing polydispersivity. Another potential drawback of working with highly polydisperse distributions is the increase in the maximum size of the filler particles which in most cases tend to govern the minimum bond line thickness (BLT) achievable by the TIMs. Also, it is important to note that that increasing the degree of polydispersivity would result in depletion of the number of filler particles near the boundaries across which heat is transported. It is crucial to ensure that there are a sufficient number of particles at these boundaries since these are the particles which "draw" the heat from the source and "drain" to the sink. However, this is not to say the bulk of the composite can be depleted of filler particles. Thus, based on the results in this paper, it can be concluded that for a given filler volume loading, an optimum σ value for polydispersivity exists beyond which the effective thermal conductivity of polymer composites starts to decrease. For a given filler volume loading, the optimum σ value is governed by

29

the trade-off between the increased thermal transport in the particle chains versus the decreasing effective surface area for thermal transport.

- The current trend in the TIM industry is summarized in Figure 18. This plot was obtained from a leading supplier of Silicone based TIMs - Shin-Etsu Chemical Company, Japan. Currently, the TIM manufacturers resort to loading the TIM formulations to as high as 80% filler volume loading to achieve superior thermal performance as seen in Figure 19. There are many drawbacks to loading the TIMs to high filler volume loadings such as:
  - ○ Increasing the filler volume loading increases the viscosity of the TIMs which in turn leads to higher BLT's.
  - ○ The difficulty with wetting of the filler particles increases as well due to the decrease in the matrix volume loading. To overcome this problem, TIM vendors tend to add volatile compounds to the matrix material which facilitate in reducing the viscosity and enhancing the wettability of the matrix to the filler materials. However, the negative impact of adding more volatile compounds is that these materials tend to evaporate during the curing of the TIMs (which is typically carried out at about $125 - 150$ ^{o}C for two hours) and create voids in the bulk of the TIM which in turn would degrade the TIM performance.

Therefore, it is important to optimize the size-distribution of the filler particles to achieve the best thermal performance at relatively lower (~60%) filler volume loading of the TIMs.

- The results shown in Figure 18 also demonstrate the limitation of the network model when used to estimate the thermal conductivity of composites at low filler volume loadings (~40 %). Since the network model estimates the effective thermal conductivity of the high-contrast composites based on the heat that is transported *only* through the filler particles, it underestimates the thermal performance of the composites at lower filler volume loadings (40% and lower). However, at higher filler loadings (50% and above) the bulk of the heat will be transported by the filler particles and the results predicted by the network model will match better to the experimental measurements.

Figure 14: Effective thermal conductivity of particulate composites at 40% filler volume loading as a function of polydispersivity parameter σ.

31

Figure 15: Effective thermal conductivity of particulate composites at 45% filler volume loading as a function of polydispersivity parameter σ.

1
2
3
4
5
6
7
8
9
10
11
12
13
14
15
16
17
18
19
20
21
22
23
24
25
26
27
28
29
30
31
32
33
34
35
36
37
38
39
40
41
42
43
44
45
46
47
48
49
50
51
52
53
54
55
56
57
58
59
60
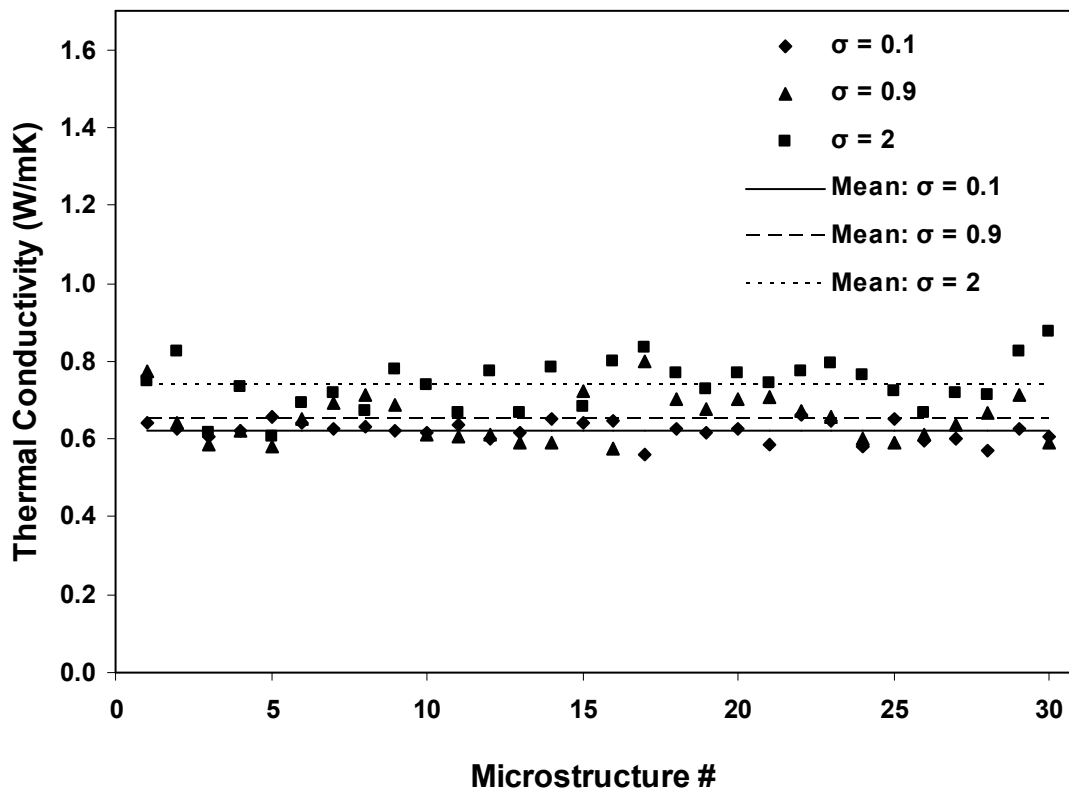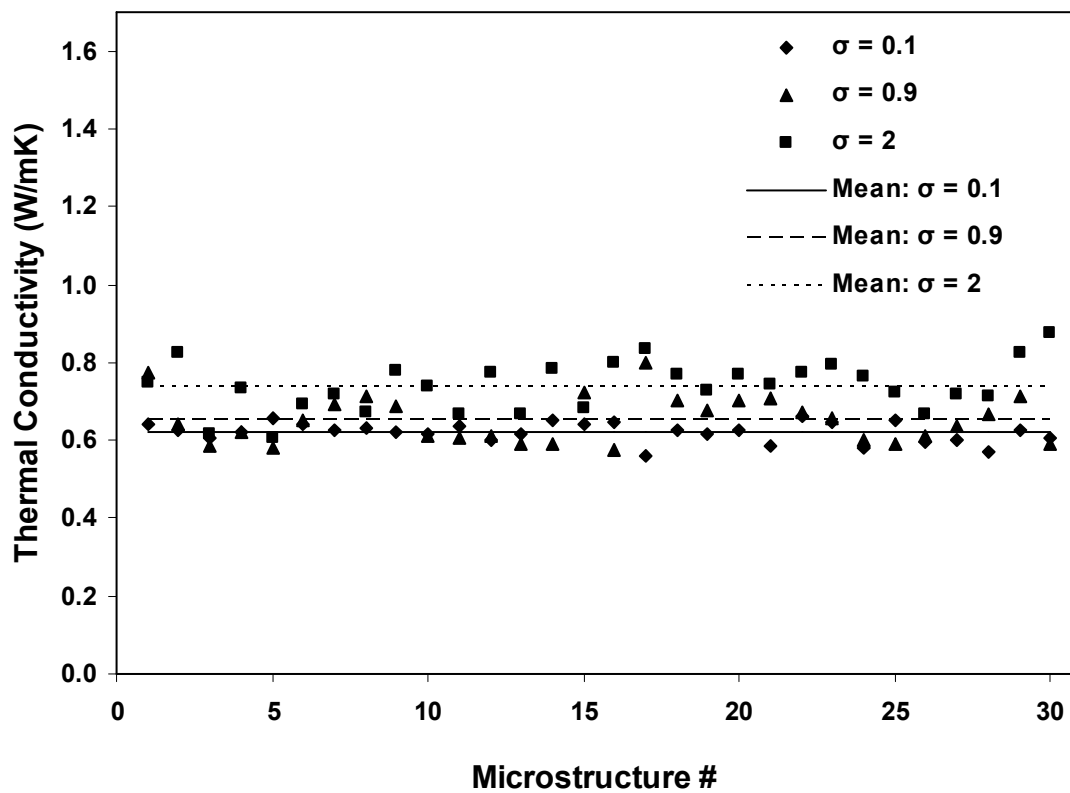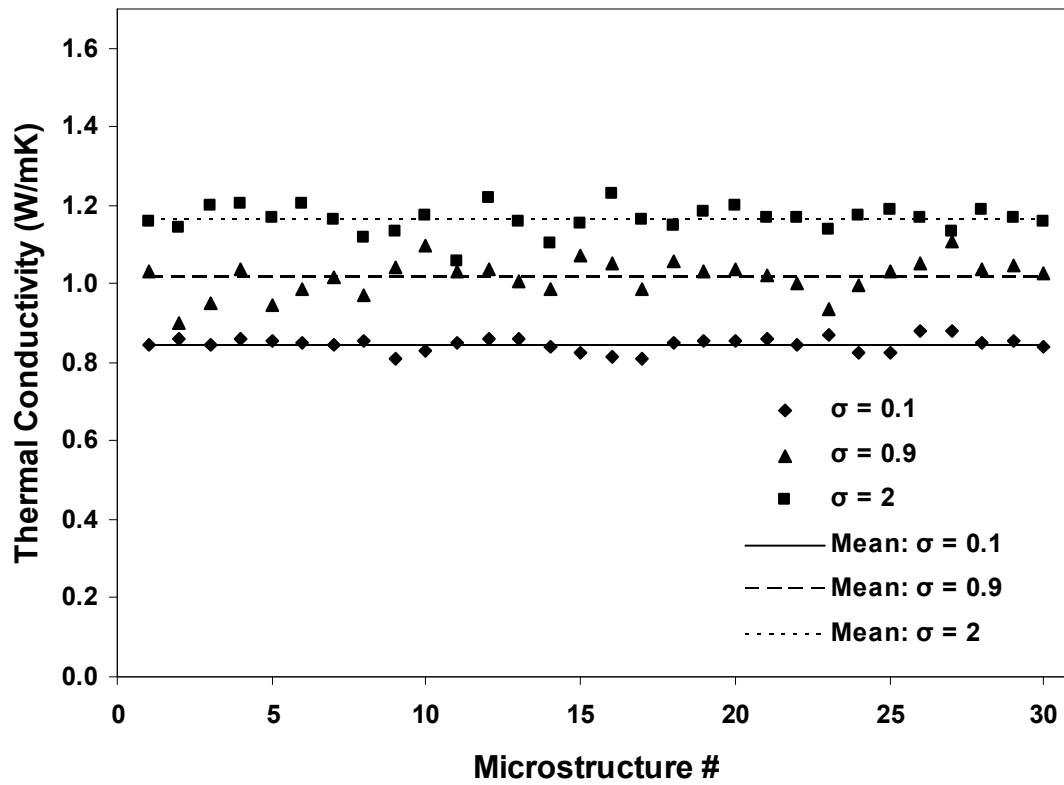

Figure 16: Effective thermal conductivity of particulate composites at 50% filler volume loading as a function of polydispersivity parameter σ.

33

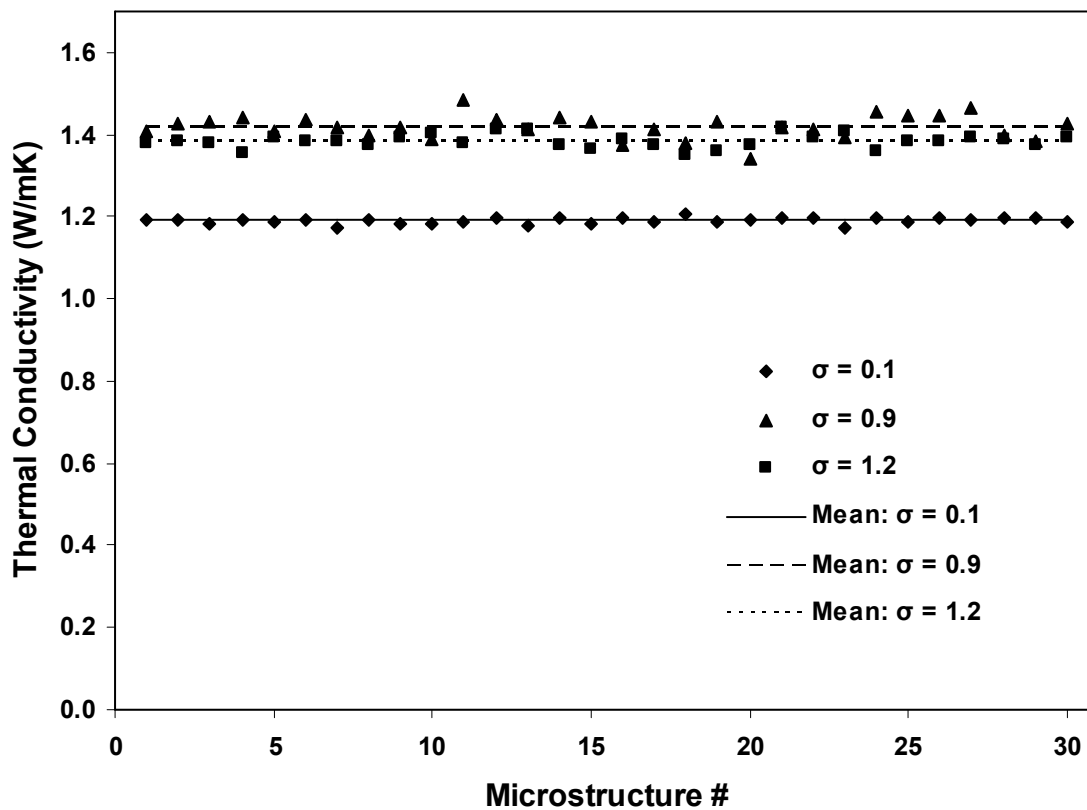Figure 17: Effective thermal conductivity of particulate composites at 55% filler volume loading as a function of polydispersivity parameter σ.

34

1
2
3
4
5
6
7
8
9
10
11
12
13
14
15
16
17
18
19
20
21
22
23
24
25
26
27
28
29
30
31
32
33
34
35
36
37
38
39
40
41
42
43
44
45
46
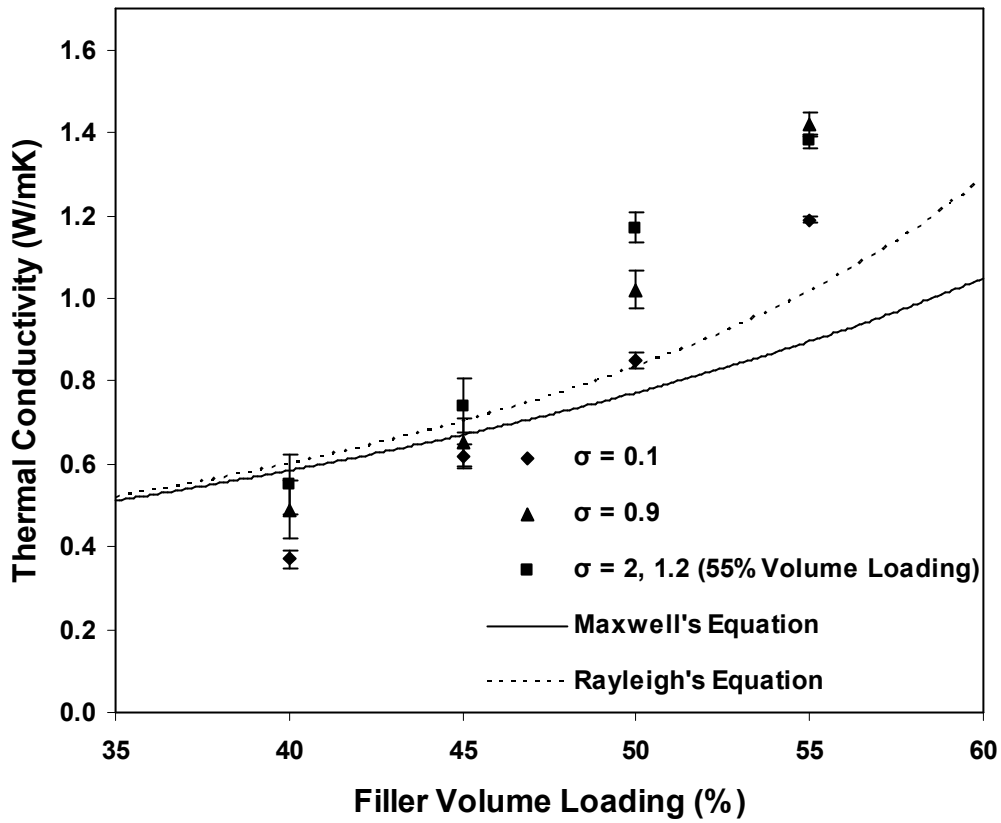47
48
49
50
51
52
53
54
55
56
57
58
59
60

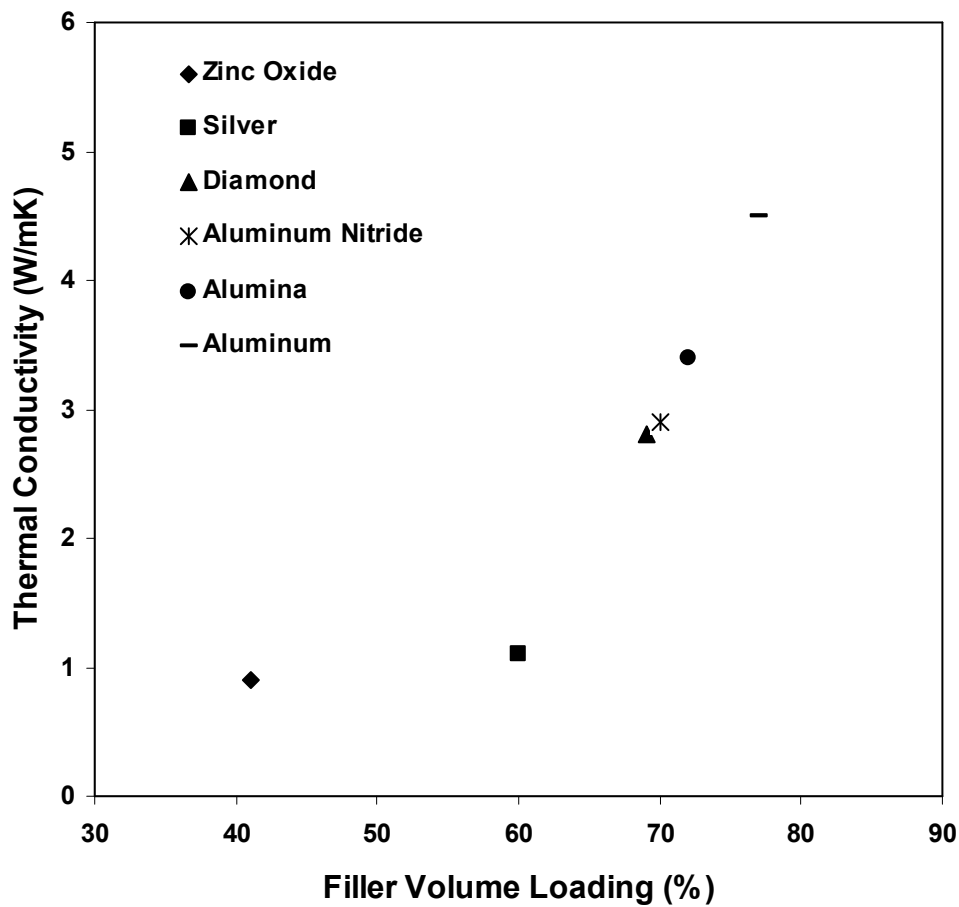Figure 18: Effect of polydispersivity on the thermal conductivity of particulate composites.

Figure 19: Effect of filler volume loading on the thermal conductivity of silicon based TIMs (Courtesy: Shin-Etsu Chemical Company, Japan).

Table 3: Effective thermal conductivity of microstructures as a function of volume loading and degree of polydispersivity σ

Filler Volume (%)	$\sigma = 0.1$ (μ_{TC}, σ_{TC}) (W/mK)	$\sigma = 0.9$ (μ_{TC}, σ_{TC}) (W/mK)	$\sigma = 2, 1.2$ (55% Volume Loading) (μ_{TC}, σ_{TC}) (W/mK)
40	(0.37, 0.02)	(0.49, 0.07)	(0.55, 0.07)
45	(0.62, 0.03)	(0.65, 0.06)	(0.74, 0.06)
50	(0.85, 0.02)	(1.02, 0.05)	(1.17, 0.04)
55	(1.19, 0.01)	(1.42, 0.03)	(1.38, 0.02)

Table 4: t-test results comparing the means of the simulated microstructures for varying degree of polydispersivity σ

Filler Volume (%)	Degree of Polydispersivity σ	Statistical t-value	Tabulated t-value	Significance Level (%)	Comment
40	0.1, 0.9	8.95			
40	0.9, 2	3.44			
45	0.1, 0.9	2.61			
45	0.9, 2	5.48	2.00	95	"Significantly" Different
50	0.1, 0.9	19.09			
50	0.9, 2	13.96			
55	0.1, 0.9	40.89			
55	0.9, 1.2	5.61			

37

Summary

The effect of polydispersivity on the effective thermal conductivity of particulate composites is elucidated in this paper. Random microstructural arrangements consisting of lognormal size-distributions of alumina particles in silicone matrix were generated and statistically characterized using the matrix-exclusion probability function. The filler particle volume loading was varied over a range of 40-55 %. For a given filler volume loading, the effect of polydispersivity in the microstructures was captured by varying the standard deviation (σ) parameter in the lognormal filler particle size distribution function. The effective thermal conductivity of the microstructures was evaluated through efficient network model simulations. Lastly, important guidelines for enhancing the thermal performance for particulate thermal interface materials are presented. Based on the results of this paper, a polydispersed system (with a controlled degree of polydispersivity) would improve effective conductivity over a uniform filler distribution. However, beyond a certain limit (which is dependent on volume fraction), increasing polydispersivity is counter-productive.

Acknowledgments

References

1. Kerstein, A. R., 1987, "Percolation Model of Polydisperse Composite Solid Propellant Combustion", *Combustion and Flame*, Vol. 69, pp. 95-112.

2 . Russel, W. B., Saville, D. A., Schowalter, W. R., 1989, Colloidal Dispersions, Cambridge University Press, Cambridge, England.

3. Rahaman, M. N., 1995, Ceramic Processing and Sintering, Marcel Dekker Inc., New York.

4. Christensen, R. M., 1979, Mechanics of Composite Materials, Wiley, New York.

5. Scheidegger, A. E., 1974, The Physics of Flow through Porous Media, University of Toronto Press, Toronto.

6. Maxwell, J. C., 1873, *Electricity and Magnetism*, 1st ed., Clarendon, Oxford.

7. Hasselman, D. P. H., Johnson, L. F., "Effective Thermal Conductivity of Composites with Interfacial Thermal Barrier Resistance", *J. Compos. Mater*., Vol. 21, pp. 508-515, 1987.

8. Nan, C. W., Birringer, R., Clarke, D. R., Gleiter, H., "Effective Thermal Conductivity of Particulate Composites with Interfacial Thermal Resistance", *J. Appl. Phys*., Vol. 81, no. 10, pp. 6692-6699, 1997.

9 . Benvensite, Y., "Effective Thermal Conductivity of Composites with a Thermal Contact Resistance between the Constituents: Non-dilute case", *J. Appl. Phys*., Vol. 61, no. 8, pp. 2840-2843, 1987.

10. Lord Rayleigh., "On the Influence of Obstacles Arranged in Rectangular Order upon the Properties of a Medium", *Phil. Mag.,* Vol. 34, pp. 481-502, 1892.

39

11. McPhedran, R. C. and McKenzie, D. R., "The Conductivity of Lattices of Spheres. I. The Simple Cubic Lattice", *Proc. R. Soc. Lond. A.*, Vol. 359, pp. 45-63, 1978.

12. McKenzie, D. R., McPhedran, R. C. and Derrick, G. H., "The Conductivity of Lattices of Spheres. II. The Body Centered and Face Centered Cubic Lattices", *Proc. R. Soc. Lond. A.*, Vol. 362, pp. 211-232, 1978.

13. Gu, G., Liu, Z., "Effects of Contact Resistance on the Thermal Conductivity of Composite Media with a Periodic Structure," *Journal of Physics D: Applied Physics*, Vol. 25, pp. 249-255, 1992.

14. Torquato, S., 2002, Random Heterogeneous Materials, Springer-Verlag, New York.

15. Bruggeman, D., "Berechnung verschiedener physikalischer Konstanten von heterogenen Substanzen", *Ann. Physik (Liepzig)*, Vol. 24, pp. 636-679, 1935.

16. Landauer, R., "The Electrical Resistance of Binary Metallic Mixtures", *J. Appl. Phys.,* Vol. 23, pp. 779-784, 1952.

17. Landauer, R., "Electrical Conductivity in Inhomogeneous Media", Electrical, Transport and Optical Properties of Inhomogeneous Media, J. C. Garland and D. B. Tanner (eds.), AIP, New York, pp. 2-43, 1978.

18. Every, A. G., Tzou, Y., Hasselman, D. P. H., Raj, R., "The Effect of Particle Size on the Thermal Conductivity of ZnS/Diamond Composites", *Acta Metall. Mater.*, Vol. 40, 1992.

19. Kanuparthi, S., Zhang, X., Subbarayan, G., Sammakia, B. G., Gowda, A. and Tonapi, S., "Full-Field Simulations of Particulate Thermal Interface Materials: Separating the Effects of Random Distribution from Interfacial Resistance", *Proc. of Itherm'06*, San Diego, May 30 – Jun 2, pp. 1276-1282, 2006.

20. Kanuparthi, S., G. Subbarayan, G., Siegmund, T., and Sammakia, B. G., "An Efficient Network Model for Determining the Effective Thermal Conductivity of Particulate Thermal Interface Materials," IEEE Transactions on Components and Packaging Technology, Vol. 31, No. 3, pp. 611-621, 2008.

21. Kanuparthi, S., Zhang, X., Subbarayan, G., Sammakia, B. G., Siegmund, T., Gowda A. and Tonapi, S., "Random Network Percolation Model for Particulate Thermal Interface Materials," In Proceedings of the 10th Intersociety Conference on Thermal and Thermomechanical Phenomena in Electronic Systems (Itherm 2006), IEEE, pp. 1192-1198, 2006.

22. Zhang, X. and Subbarayan, G., "jNURBS: An Extensible Symbolic Object-Oriented Framework for Integrated Mesh-less Analysis and Optimal Design", *Advances in Engineering Software*, Vol. 37, No. 5, pp. 287-311, 2006.

23. Schulz, G. V., "Uber die Kinetic der Kettenpolymerisationen", *Z. Physik Chem.*, Vol. B43, pp. 25-46, 1939.

24. Cramer, H., 1954, <u>Mathematical Method of Statistics</u>, Princeton University Press, Princeton.

25. Stroeven, P., Stroeven, M., "Assessment of Packing Characteristics by Computer Simulation", *Cement and Concrete Research*, Vol. 29, No. 8, pp. 1201-1206, 1999.

41

26 . Smith, L., Midha, P., "A Computer Model for Relating Powder Density to Composition, Employing Simulations of Dense Random Packings of Monosized and Bimodal Spherical Particles", *Journal of Material Processing Technology*, Vol. 72, pp. 277-282, 1997.

27. Zhang, X., 2004, Constructive Modeling Strategies and Implementation Frameworks for Optimal Hierarchical Synthesis, Ph.D. Thesis, Purdue University, West Lafayette, IN, USA.

28. Lu, B., and Torquato, S., "Nearest-Surface Distribution Functions for Polydispersed Particle Systems," *Physical Review A*, Vol. 45, No. 8, pp. 5530-5544, 1992.

29. Batchelor, G. K. and O'Brien, R. W., "Thermal or Electrical Conduction through a Granular Material", *Proceedings of the Royal Society of London. Series A, Mathematical and Physical Sciences*, Vol. 355, No. 1682, 313-333, 1977.

30. Elsayed, E. A., 1996, "Reliability Engineering," Addison Wesley Longman, Inc., Reading, MA.

Author Biographies:
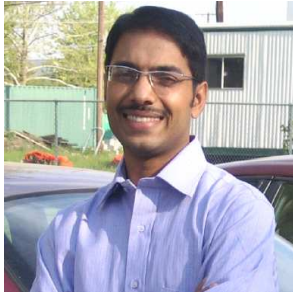
Dr. Sasanka Kanuparthi is a Senior Engineer at Amkor Technology. He received his Bachelors in Technology in Chemical Engineering from Indian Institute of Technology, Chennai, India in 2000. He received his Masters and Doctorate in Mechanical Engineering from Purdue University in 2002 and 2007, respectively. Dr. Kanuparthi is a recipient of the Itherm 2008 Outstanding Paper Award in the thermal management track. His research interests include Experimental and Computational Heat Transfer, Thermal Management of Microelectronics, Design of Thermal Systems and Design of Nano-composites.

Dr. Ganesh Subbarayan is a Professor of Mechanical Engineering at Purdue University. He was previously at University of Colorado (1994-2002) and at IBM Corporation (1990-1993). He holds a B.Tech degree in Mechanical Engineering (1985) from the Indian Institute of Technology, Madras and a Ph. D. (1991, direct PhD program) degree in Mechanical Engineering from Cornell University. Dr. Subbarayan's research is in Computational Modeling and Design of objects over multiple length scales with applications to reliability of Microelectronic Interconnects and Packages. Dr. Subbarayan is a recipient of the 2005 Mechanics Award from the ASME EPP Division, 2005 University Faculty Scholar Award from Purdue University, NSF CAREER award, the NSF Research Initiation Award, the 2003 Charles E. Ives Outstanding Paper Award from the Journal of Imaging Science and Technology, the 2002 Highly Commended Award

43

from Soldering and Surface Mount Technology journal, the Itherm 2000 Best Paper Award, the 1996 Peter A. Engel Best Paper Award from ASME Journal of Electronic Packaging, and an IBM Invention Achievement Award. He has served on the program committees of several conferences including the ASME/Pacific Rim International Intersociety Conferences on Electronics Packaging (1997 program co-chair, 1999 reliability track chair, 2001 Modeling and Characterization track chair), ASME International Mechanical Engineering Conference and Exhibition (2002 Program Chair, EPP Division) and Intersociety Conference on Thermal and Thermomechanical Phenomenon in Electronic Systems (2002 program co-chair, Mechanics). He is a Fellow of ASME and he currently serves as the Editor-in-Chief of IEEE Transactions on Advanced Packaging.

Dr. Thomas Siegmund is Professor of Mechanical Engineering at Purdue University. He holds a Diplom Ingenieur (1990) and Doctorate (1994) from the University of Leoben, Austria. His research interests are in computational solid mechanics, biomechanics and manufacturing systems. Dr. Siegmund is a Purdue University Faculty Scholar (2004), a recipient of the 2002 Best Paper Award of the American Society of Composites. From 1997-1999 he was a Lecturer of the Federation of European Materials Societies (FEMS), and from 1995-1996 a recipient of the Erwin Schrödinger Fellowship, Austrian Science Foundation. He contributed to the organizational structure of several conferences including the 2008 International Congress of Technical and Applied Mechanics, the 2006 and 2008 Annual Technical Meetings of the Society of Engineering Science, and has been a lecturer at the International Center Mechanical Sciences (CISM) in Udine, Italy.

1
2
3
4
5
6
7
8
9
10
11
12
13
14
15
16
17
18
19
20
21
22
23
24
25
26
27
28
29
30
31
32
33
34
35
36
37
38
39
40
41
42
43
44
45
46
47
48
49
50
51
52
53
54
55
56
57
58
59
60

Dr. Bahgat Sammakia is Director of the Integrated Electronics Engineering Center. Bahgat Sammakia received his Bachelor of Science degree in Mechanical Engineering in 1977, from the University of Alexandria in Egypt. He received the masters and doctorate degrees in mechanical engineering in 1980 and 82 respectively from the State University of New York at Buffalo. His research work was in the areas of natural convection heat transfer. After graduating from SUNY, Bahgat worked at the University of Pennsylvania as a postdoctoral fellow.

Bahgat joined IBM in 1984 as an engineer in the thermal management area. In 1985 he was promoted to manager of the thermal management department. Bahgat continued to work in IBM until 1998, in various management positions, including managing the thermal and mechanical analysis groups, the surface science group, the chemical lab, the site technical assurance group, and his last position in IBM was manager of development for organic packaging in the IBM Microelectronics division.

Bahgat holds seven US patents and twelve IBM technical disclosures; he has published over 50 technical papers in refereed journals and conference proceedings. Bahgat has contributed to three books on natural convection heat transfer and electronic packaging.

45